ELSEVIER

Spatial uncertainty analysis of population models

Henriette I. Jager[a,*], Anthony W. King[a], Nathan H. Schumaker[b],
Tom L. Ashwood[a], Barbara L. Jackson[a]

[a] *Oak Ridge National Laboratory, Environmental Sciences Division, Bethel Valley Road, Oak Ridge, TN 37831-6036, USA*
[b] *US Environmental Protection Agency, Corvallis, OR, USA*

Abstract

This paper describes an approach for conducting spatial uncertainty analysis of spatial population models, and illustrates the ecological consequences of spatial uncertainty for landscapes with different properties. Spatial population models typically simulate birth, death, and migration on an input map that describes habitat. Typically, only a single "reference" map is available, but we can imagine that a collection of other, slightly different, maps could be drawn to represent a particular species' habitat. As a first approximation, our approach assumes that spatial uncertainty (i.e., the variation among values assigned to a location by such a collection of maps) is constrained by characteristics of the reference map, regardless of how the map was produced. Our approach produces lower levels of uncertainty than alternative methods used in landscape ecology because we condition our alternative landscapes on local properties of the reference map. Simulated spatial uncertainty was higher near the borders of patches. Consequently, average uncertainty was highest for reference maps with equal proportions of suitable and unsuitable habitat, and no spatial autocorrelation. We used two population viability models to evaluate the ecological consequences of spatial uncertainty for landscapes with different properties. Spatial uncertainty produced larger variation among predictions of a spatially explicit model than those of a spatially implicit model. Spatially explicit model predictions of final female population size varied most among landscapes with enough clustered habitat to allow persistence. In contrast, predictions of population growth rate varied most among landscapes with only enough clustered habitat to support a small population, i.e., near a spatially mediated extinction threshold. We conclude that spatial uncertainty has the greatest effect on persistence when the amount and arrangement of suitable habitat are such that habitat capacity is near the minimum required for persistence.
Published by Elsevier B.V.

Keywords: Geostatistics; Conditional simulation; Population viability; Extinction threshold; Spatial life history

1. Introduction

Environmental variability (spatial and temporal) is a critically important feature of natural systems, and should not be neglected in ecological models (Cormack, 1988). Even in the absence of temporal

* Corresponding author. Tel.: +1 865 574 8143;
fax: +1 865 576 3989.
E-mail address: jager@ornl.gov (H.I. Jager).
URL: http://www.esd.ornl.gov/~zij.

variation, spatial structure can have a strong influence on the dynamics of populations (Ritchie, 1997). This is why models used for population viability analysis (PVA) typically include environmental variation to assess a population's chances for persisting into the future. Spatially explicit population models (e.g., Dunning et al., 1995) are often used in PVA when the populations of concern inhabit spatially heterogeneous landscapes.

1.1. Monte Carlo analysis of spatial models

Spatially explicit population models require geo-referenced input data about habitat (e.g., vegetation, soil, habitat suitability). The influence of uncertainty in the values provided as spatial inputs on model predictions is, therefore, a concern (e.g., Hansen et al., 1999; Bennett et al., 2000; Hunsaker et al., 2001; Elith et al., 2002). Understanding the effects of these spatial inputs adds a new wrinkle to the process of model testing and evaluation.

Population models are expected to go through uncertainty and sensitivity analysis as part of their development and testing (McCarthy et al., 1995; Bart, 1995). Sensitivity analysis ranks parameters according to their relative influence on model predictions, whereas uncertainty analysis quantifies the variation in model predictions due to variation in parameters. The purpose of sensitivity analysis is to identify key parameters for more careful measurement in the hope of reducing uncertainty. The purpose of uncertainty analysis is to provide confidence limits on model predictions. Existing tools to evaluate non-spatial models in ecology (e.g., Gardner et al., 1981) are now being supplemented by others that are capable of dealing with spatial inputs.

Tools for spatial uncertainty analysis answer the question, "Given the variation known to exist among realistic alternative landscapes, how variable are model predictions?" This question is answered by generating alternative landscapes, using each one as input to the population model of interest, and quantifying the variation among model predictions. Alternative landscapes are often generated using a statistical model that serves as a caricature of spatial variation in model inputs. In the ecological literature, alternative landscapes have often been produced using fractal models that impose very little constraint and result in very different realizations (e.g., With and King, 2001; Gardner

and Gustafson, 2004). Geostatistical models provide an alternative that results in more-realistic alternative maps. Geostatistical models assume that spatial uncertainty is controlled by the average statistical properties (e.g., mean, variance–covariance, and spatial autocorrelation) of the landscape. Describing spatial autocorrelation is, therefore, an important aspect of spatial uncertainty analysis. Heuvelink (1998) demonstrated spatial uncertainty analysis for continuous data. In this paper, we outline an approach that uses a geostatistical model to simulate spatial uncertainty in multinomial data.

Here, we describe a method for spatial uncertainty analysis that constrains the generated landscapes to share certain properties of a reference map, including (1) the average proportion of different habitat categories, (2) the spatial autocorrelations among categories, and (3) local fidelity at a regular grid of locations. We generate alternative maps by conditioning multinomial probabilities used to classify each location on the surrounding data. Because values are conditioned on a coarse grid from the reference map, our approach produces a more realistic, less variable, collection of alternative maps than those produced using null landscape generators such as RULE. Our method preserves large-scale features that would be unlikely to change in different renditions of a map. To illustrate our approach, we focus on binary habitat maps used as input to population models.

Our main goal is to demonstrate a method for spatial uncertainty analysis of population viability models. Our secondary objective is to begin to understand what species attributes and landscape properties make animal population models sensitive to spatial uncertainty.

1.2. Representing spatial life histories using a population model

The spatial life history of a species influences the ability of its populations to persist in different landscapes. Similarly, the sensitivity of a spatial population model to spatial uncertainty may depend, in part, on the spatial life history of the species represented.

Two main features of a species' spatial life history are its habitat requirements and its movement patterns. To demonstrate our technique, we use two spatial population models to compare hypothetical species that differ in spatial life history. A source–sink model
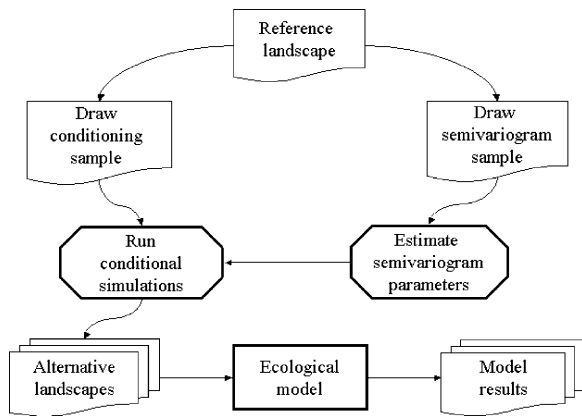
Fig. 1. Flow chart of the procedure for generating alternative landscapes for spatial uncertainty analysis.

is used to compare species that differ in habitat requirements: one species that requires edge habitat and one species that requires interior habitat. We expect that edge-dependent species will be more sensitive to changes in the size and shape of habitat patches associated with spatial uncertainty than interior species. A spatially explicit model is used to compare species with high and low mobility. We expect that a mobile species that integrates over the landscape in a course-grained manner will be less sensitive to spatial uncertainty than a less-mobile species that uses the landscape in a fine-grained manner (Levins, 1968).

2. Methods

Our approach to spatial uncertainty analysis is depicted in Fig. 1 and described in four sections below. Normally, a reference landscape would be the starting point for spatial uncertainty analysis. Because this paper explores the implications of using a reference map with different spatial statistical properties, we generated reference maps with known properties. We describe our methods for generating these reference landscapes in the first section below. The second section below describes the generation of alternative landscapes from a reference map. The third section describes how we quantified the resulting spatial uncertainty. The fourth section describes the propagation of spatial uncertainty through each of two population models, and our methods for summarizing results.

All of the geostatistical methods described here were implemented using GSTAT (Pebesma and Wesseling, 1998; http://www.frw.ruu.nl/gstat/).

2.1. Generation of reference landscapes

We began by producing original reference landscapes with known spatial–statistical properties (Fig. 2). We studied six different reference landscapes to better understand how the frequency of suitable habitat, p, and the degree of spatial autocorrelation, C, influence spatial uncertainty. Each reference map was created by producing a single unconditional simulation from the random model in Eq. (1), with the values of p and C shown in Table 1. For some analyses, we also produced maps with $p = 0.9$ (suitable habitat is common) by switching suitable and unsuitable categories in maps with $p = 0.1$ (suitable habitat is rare).

Each reference landscape was generated on a 500×500 grid, with a grid cell size of $20\,\text{m} \times 20\,\text{m}$. We assigned each cell a habitat type with two possible values, $I = 0$ (unsuitable) or 1 (suitable).

We used unconditional simulation (Burgess and Webster, 1980) to generate each reference map. Unconditional simulation of categorical data requires a mean frequency, p, and a semivariogram model, $\gamma(h)$ that describes the probability that pairs of locations separated by distance h belong to the same category, or in our case, that they are both either suitable or not.

We adopted an exponential semivariogram with a range parameter fixed at 1000 m, nugget parameter θ_1, and sill parameter θ_2. The ratio $C = \theta_2/(\theta_1 + \theta_2)$ describes the degree of spatial autocorrelation.

$$\gamma(h) = \theta_1 + \theta_2 \left(1 - \exp\left(\frac{-h}{1000} \right) \right), \quad h > 0$$
$$\theta_1 + \theta_2 = \text{Var}(I) = p(1 - p) \tag{1}$$

2.2. Generation of alternative landscapes

We assume that spatial uncertainty is constrained by the spatial properties of the reference map. In practice, we would be handed a reference map without knowing the underlying process and parameters that generated it. Therefore, we pretend the parameter values are unknown and begin by estimating parameter values from the reference map, as described in Section 2.2.1 below. Next, we generate a sample of alternative landscapes
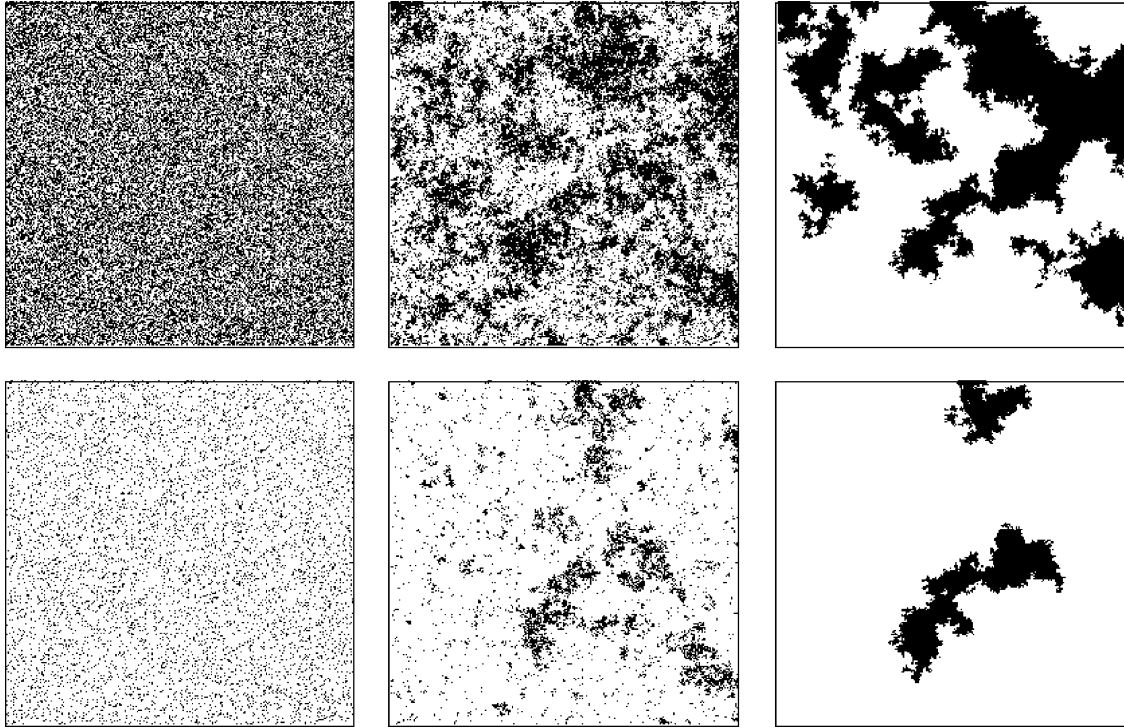
Fig. 2. Reference landscapes generated for each of six scenarios. White areas are locally unsuitable for all species. The proportion of suitable habitat in landscapes is $p = 0.5$ in the top row and $p = 0.1$ in the bottom row. The degree of spatial autocorrelation increases from left to right ($C = 0$, 0.5, and 1).

using conditional simulation (Section 2.2.2). These landscapes share the global spatial–statistical properties of the reference map, as well as local features from a subset of locations.

2.2.1. Spatial autocorrelation

To characterize each reference map, we estimate the proportion of cells with suitable habitat and spatial au-tocorrelation. To describe the latter, we estimate parameters of an exponential semivariogram model from a sample drawn from each reference map. We designed the semivariogram sample (Fig. 1) to characterize au-tocorrelation well for short separation distances (where autocorrelation and predictive value is high) and to obtain uniform spatial coverage. A stratified, random sampling design that combined a sample of points from

Table 1
Experimental design to evaluate the role of reference map characteristics

Mean frequency of category		Spatial autocorrelation		
$I = 0$	$I = 1$	None ($C = 0$)	Moderate ($C = 0.5$)	Strong ($C = 1$)
0.1 (rare)	0.9	$\theta_1 = 0.09$ $\theta_2 = 0.0$	$\theta_1 = 0.045$ $\theta_2 = 0.045$	$\theta_1 = 0.0$ $\theta_2 = 0.09$
0.5 (half)	0.5	$\theta_1 = 0.25$ $\theta_2 = 0.0$	$\theta_1 = 0.125$ $\theta_2 = 0.125$	$\theta_1 = 0.0$ $\theta_2 = 0.25$

Values of two variogram parameters, θ_1 (nugget) and $\theta_1 + \theta_2$ (sill), and C (ratio of θ_2 to sill) are given for each of the six landscape types.

a regular, coarse grid with a sample of randomly drawn neighbors addresses both criteria (Warrick and Meyers, 1987).

Next, we fit one semivariogram model to the sample data for $I=0$ (unsuitable habitat) and another for $I=1$ (suitable habitat). We specified an exponential model with the known range of 1000 m and used GSTAT to estimate the remaining semivariogram parameters. Iteratively reweighted least squares (Neuman and Jacobson, 1984; Cressie, 1985) estimates the sill and nugget parameters by minimizing

$$\sum_{i=1}^{20} w_i(\hat{\gamma}(h_i) - \gamma(h_i))^2, \quad \text{where } w_i = \frac{N_i}{\gamma(h_i)}. \quad (2)$$

The semivariogram fit improved when we excluded data pairs farther apart than half the range. This 500-m distance was divided evenly into 20 intervals, i. Larger weights, w_i, were assigned to intervals with (1) more pairs of sample locations and (2) with less variability. For all six scenarios, we set the initial parameter estimates for θ_1 and θ_2 to the true parameter values from Table 1. We used semivariogram models with these parameter estimates in generating each of the alternative landscapes.

2.2.2. Stochastic simulation

We used stochastic simulation (see Rossi et al., 1993) to produce a sample of 10 alternative landscapes sharing the spatial–statistical qualities of each reference map. This relatively small collection does a reasonable job of describing variation produced by our method, and simplifies our presentation for illustrative purposes. Stochastic simulation produces a collection of rough surfaces (realizations) that reproduce the variability in a spatial field (Journel and Huijbregts, 1978). The mean of many realizations is the smoothed kriged surface.

Simulated surfaces can be conditioned on available data, forcing each surface to converge to measured values at sampled locations. Conditioning produces landscapes with a closer resemblance to the reference map than unconditional simulation. The density of the conditioning sample (Fig. 1) controls the degree of realism in alternative maps. Simulations with a larger proportion of pixels sampled from the reference map have lower variability. We conditioned our simulations on a 3% conditioning sample drawn uni-

formly at random from the reference map (i.e., the starting cell was drawn at random from the top-left corner; from that point the placement of the rest of the sample grid was fixed). We chose a small percentage because preliminary simulations with higher conditioning sample sizes showed very little variation among replicate landscapes.

The simplest way to understand stochastic simulation is to think of adding a random normal deviate to the kriged mean surface, where the deviate drawn at each location has zero as its mean and the kriging variance as its variance. We used a sequential simulation algorithm (Gotway and Rutherford, 1994; Gomez-Hernandez and Cassiraga, 1994) because it is computationally efficient and can be used with any type of variable and distribution (Bierkens and Burrough, 1993). Each realization is drawn from a multivariate probability distribution function where every location has its own random variable. Through repeated application of Bayes' theorem, the multivariate distribution is constructed at each newly simulated location as a product of univariate conditional simulations. Once the value at a location is simulated, it is added to the conditioning data for a given realization. For the special case of categorical spatial data, the appropriate method is sequential indicator simulation (Gomez-Hernandez and Srivastava, 1990; Isaaks, 1984).

2.3. Quantifying spatial uncertainty

We define spatial uncertainty as the variance among habitat values assigned to the same location by a collection of alternative maps. Because our binary maps represent habitat quality, we present maps showing the variance in habitat quality ($I=0$ or 1) among replicate landscapes. By extension, spatial uncertainty among habitat maps with more than two categories could be quantified by the evenness in the distribution of categories (e.g., habitat types) assigned to a particular location by replicate maps (see Jager and King, 2004).

2.4. Propagating spatial uncertainty

The goal of spatial uncertainty analysis is to assess the variation in model predictions that result from spatial variation in inputs. The simplest models of population viability assume that population size tracks the amount of suitable habitat (e.g., Harris et al., 1992).

Therefore, we first calculate variation in the amount of suitable habitat provided by each alternative landscape.

Next, we evaluate consequences of spatial uncertainty using two population models that address different aspects of the spatial life history of species. Both models are described in Appendix A. The source–sink model distinguishes between the amount of source and sink habitat and their influence on birth, death, and migration, but it does not consider their spatial arrangement. This model cannot, therefore, reveal the effects of spatial uncertainty on mobility, but it is well suited for comparing edge-dependent and interior species.

The second model, Program to Assist in Tracking Critical Habitat (PATCH), is a spatially explicit, individual-based population model (Appendix A). The PATCH model does not simulate juxtapositional habitat requirements (i.e., edge-dependent versus interior), but it is well suited for comparing interior species with

low and high mobility. The population responses simulated by each model are described in Appendix A.

3. Results

The results presented here include the amounts of spatial uncertainty produced for landscapes with different characteristics, and the variation in predictions made by the two population models due to spatial uncertainty in spatial inputs.

3.1. Spatial uncertainty

Spatial uncertainty, defined as the variance in habitat quality among replicate maps, was highest at the boundaries of patches (black in Fig. 3) and lowest in the center of patches (white in Fig. 3). This can best be seen by comparing the areas of high spatial uncertainty
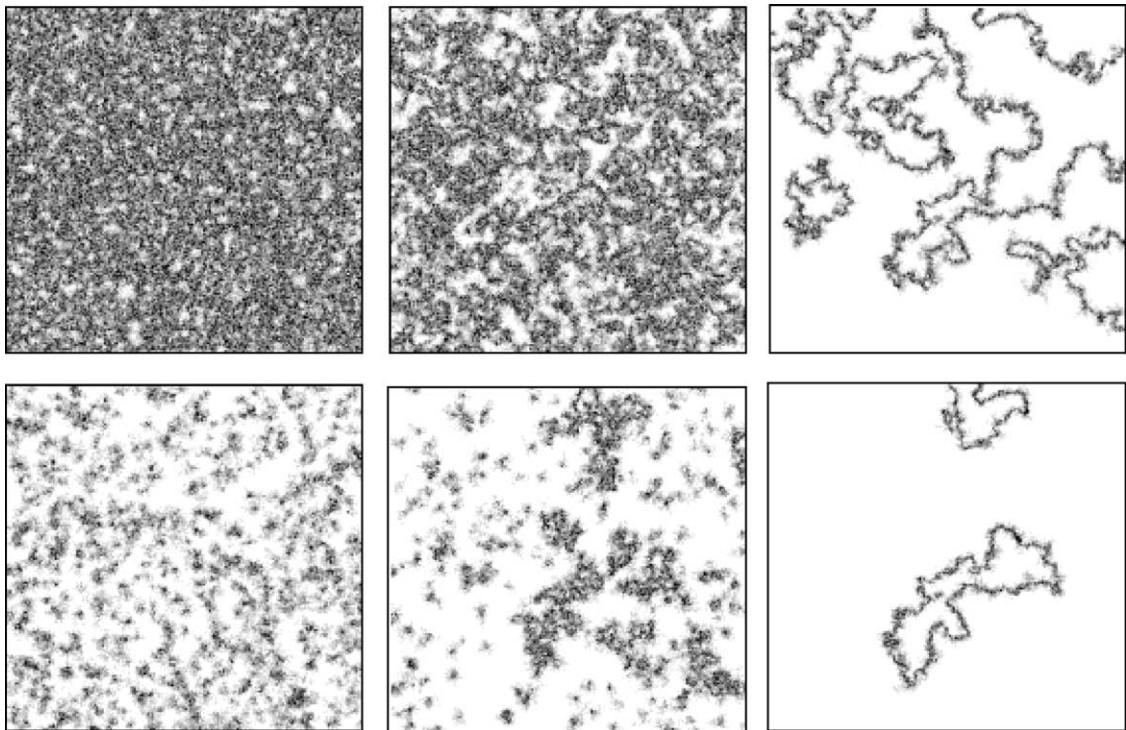

Fig. 3. Maps of spatial uncertainty for each of six scenarios. The proportion of suitable habitat in landscapes is $p = 0.5$ in the top row and $p = 0.1$ in the bottom row. The degree of spatial autocorrelation increases from left to right ($C = 0$, 0.5, and 1). Uncertainty is highest in locations designated as suitable in half of the replicate maps (black). Uncertainty is lowest in locations with either suitable or unsuitable habitat in all of the replicate landscapes (white).

in Fig. 3 with the locations of patches of suitable habitat (black) in Fig. 2.

Fig. 4 summarizes the average and S.D. of spatial uncertainty among cells for maps with different properties. Average variation among our binary habitat maps was highest when half of the replicate maps were unsuitable ($I = 0$), as illustrated by maps in the top row of Fig. 3 and the right side of Fig. 4. This is to be expected because the variance of a binomial variable reaches a maximum of 0.25 when exactly half of the replicates belong to one category and the other half belong to the other value.

Average spatial uncertainty was also higher in uncorrelated landscapes (maps in left-most column of Fig. 3 and open bars in Fig. 4) than in landscapes with high spatial autocorrelation (right-most column of Fig. 3 and black bars in Fig. 4).

We also looked at the reclassification rate for one particular category. For example, the reclassification rate for suitable habitat is the proportion of cells suitable in the reference map that were classified as unsuitable in replicate maps. Like spatial uncertainty, the average reclassification rate for one category was higher in uncorrelated landscapes than in correlated landscapes. Unlike spatial uncertainty, the rate of reclassification for a particular category was highest when the category was rare in the reference map.
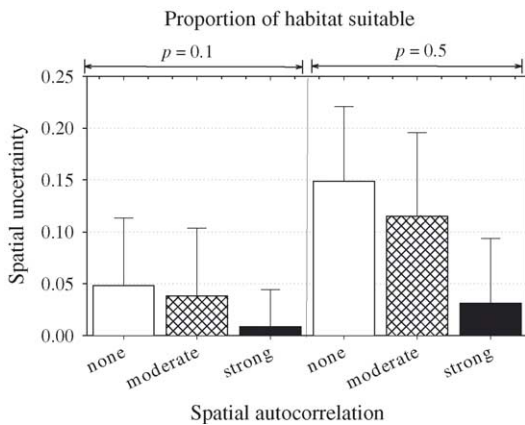
3.2. Predictions of the source–sink model

Variation among replicate landscapes in the proportion of source habitat predicted by the source–sink model was small for all species and landscape types (Table 2). This is shown by the lack of vertical scatter among points (each point is the result for one landscape) in Fig. 5a.

Overall population growth rates, λ, predicted by the source–sink model (see Appendix A) were also insensitive to differences among replicate landscapes. The largest standard deviation in λ among 10 replicate landscapes was less than 0.04 (Table 3). However, near the population growth rate threshold ($\lambda = 1$) this small variation among landscapes can have important consequences. For some replicate landscapes, the population model predicts overall population increase ($\lambda > 1$); in
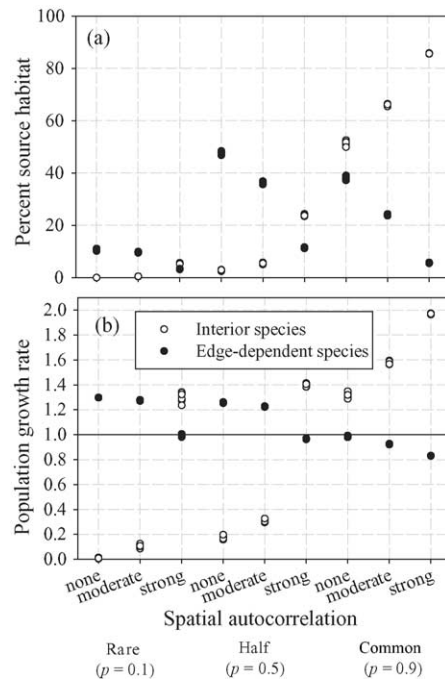

Fig. 5. Predictions of (a) percent source habitat and (b) population growth rate were generated by the source–sink model for an interior species and an edge-dependent species on ten replicate landscapes in each of nine landscape categories. Landscape categories included three proportions of suitable habitat: common ($p = 0.9$), half ($p = 0.5$), and rare ($p = 0.1$), and three levels of spatial autocorrelation: none, moderate, and strong.

Fig. 4. Average spatial uncertainty, measured as the S.D. of I-values among replicate landscapes, averaged across map cells. Individual bars show average values for reference maps differing in the proportion of suitable habitat, p, and the degree of spatial autocorrelation (error bars show among cell variation = 1 S.D.).

Table 2
Standard deviation in the percent of source habitat predicted by the source–sink model for two species types and nine landscape types

Proportion suitable	Species type	Degree of spatial autocorrelation		
		None	Moderate	Strong
0.1	Interior	0.0179	0.0521	0.2309
	Edge-dependent	0.3687	0.2156	0.1038
0.5	Interior	0.3954	0.1792	0.2847
	Edge-dependent	0.6441	0.4587	0.1706
0.9	Interior	0.9463	0.5188	0.1397
	Edge-dependent	0.6618	0.3615	0.1381

Note that we produced maps with switched suitable and unsuitable use the maps in which suitable habitat has an expected frequency $p = 0.9$ by switching $I = 0$ to 1, and vice versa, in maps with $p = 0.1$.

Table 3
Standard deviation in overall population growth rate predicted by the source–sink model for two species types and nine landscape types

Proportion suitable	Species type	Degree of spatial autocorrelation		
		None	Moderate	Strong
0.1	Interior	0.0034	0.0117	0.0358
	Edge-dependent	0.0008	0.0028	0.0085
0.5	Interior	0.0139	0.0085	0.0106
	Edge-dependent	0.0033	0.0020	0.0025
0.9	Interior	0.0178	0.0093	0.0031
	Edge-dependent	0.0042	0.0022	0.0007

Note that we produced maps with switched suitable and unsuitable use the maps in which suitable habitat has an expected frequency $p = 0.9$ by switching $I = 0$ to 1, and vice versa, in maps with $p = 0.1$.

others, the model predicts that the population will decline ($\lambda < 1$) to extinction (Fig. 5b).

Interior and edge-dependent species showed different responses to reference landscape properties. The interior species derived more source habitat and faster population growth from landscapes with more suitable habitat and strong spatial autocorrelation, whereas the edge-dependent species performed best on landscapes with equal amounts of suitable and unsuitable habitat and no autocorrelation (Fig. 5). However, as noted above, spatial uncertainty had little impact on population growth rates.

3.3. Predictions of the PATCH model

Spatial uncertainty produced more variation in predictions of the PATCH model than in predictions of the source–sink model. Variation among individual replicates is shown in Fig. 6a and b, and the S.D. in two predictions (see Appendix A), final female population, N_f and population growth rate are shown in Table 4.

Variation in N_f was higher for landscape types with a high carrying capacity, i.e., more suitable habitat ($p = 0.5$) and/or higher spatial autocorrelation. The S.D. in N_f was higher for populations simulated on landscapes types with higher average N_f and no extinctions (S.D. > 180 in Table 4) than for those simulated on landscape types on which some replicates reached extinction (S.D. < 90 in Table 4).

In contrast to the results for N_f, variation in population growth rate (Fig. 6b) was greatest for landscape types with a low carrying capacity, suggested by a low average N_f (Fig. 6a). Depending on spatial details of a particular replicate map, populations might saturate breeding territories or decline to extinction. The S.D. in average population growth rate was zero in landscape types on which no populations persisted; low (0.005–0.02) in landscape types that had no extinctions; and high (0.05–0.45) in landscape types with extinctions for some replicate simulations (Table 4). Spatial uncertainty caused the highest variation among predictions of population growth in landscape types with

Table 4
Results predicted by the spatially explicit model for two species types and six landscape types

Proportion suitable	Species type	Degree of spatial autocorrelation		
		None	Moderate	Strong
Proportion persisting, P				
0.1	Non-mobile	0.0	0.8	1.0
	Mobile	0.0	1.0	1.0
0.5	Non-mobile	1.0	1.0	1.0
	Mobile	1.0	1.0	1.0
S.D. in final female number, N_f				
0.1	Non-mobile	0.0	66.7	184.3
	Mobile	0.0	87.4	232.7
0.5	Non-mobile	264.6	327.8	267.4
	Mobile	262.9	228.6	330.0
S.D. in population growth rate				
0.1	Non-mobile	0.0	0.438	0.015
	Mobile	0.0	0.094	0.017
0.5	Non-mobile	0.059	0.027	0.010
	Mobile	0.057	0.022	0.006

small average N_f ($p = 0.1$, moderately correlated landscapes for mobile and less-mobile species and $p = 0.5$, uncorrelated landscapes for the less-mobile species in Fig. 6a and b).

On average, populations of the mobile species attained larger final female sizes than those of the less-mobile species (Fig. 6a). The mobile and less-mobile species showed a similar response to spatial uncertainty, except in one case where the difference in average N_f placed one species closer to an extinction threshold. For landscapes with $p = 0.5$ and no autocorrelation, the N_f predictions for the non-mobile species were much nearer zero than those for the mobile species (Fig. 6a); therefore population growth rates of the non-mobile species varied more (Fig. 6b). Populations of the less-mobile species reached extinction within 500 years in two replicate landscapes (Fig. 7a), but all populations of the mobile species persisted (Fig. 7b). We do not attribute this difference in the effect of spatial uncertainty to species mobility, but rather to the proximity of average N_f predictions to zero. If we had simulated a lower proportion of suitable habitat, say $p = 0.05$, perhaps populations of the less-mobile species would have gone uniformly extinct and the mobile species would have produced the more variable response of the two.

4. Discussion

The main goal of this study was to demonstrate a method for spatial uncertainty analysis of population models, as discussed in Sections 4.1 and 4.2 below. The case studies did not use very many replicate landscapes or population models, and can therefore only suggest patterns. Although preliminary, our results begin to understand what species attributes and landscape properties make animal population models sensitive to spatial uncertainty. We discuss these results in Section 4.3 below.

4.1. Generation of alternative landscapes

One feature that distinguishes landscapes generated by this method from null landscapes is that they honor the spatial statistical properties of the original reference landscape. To draw an analogy with painting, a random map is non-representational, modern art, whereas each of our maps is an impressionist's rendering of the original landscape. Maps produced for the purpose of error analysis are meticulously generated reproductions obtained by analyzing and modeling variations among paintings of the same landscape by different artists. By sharing properties at a small subset
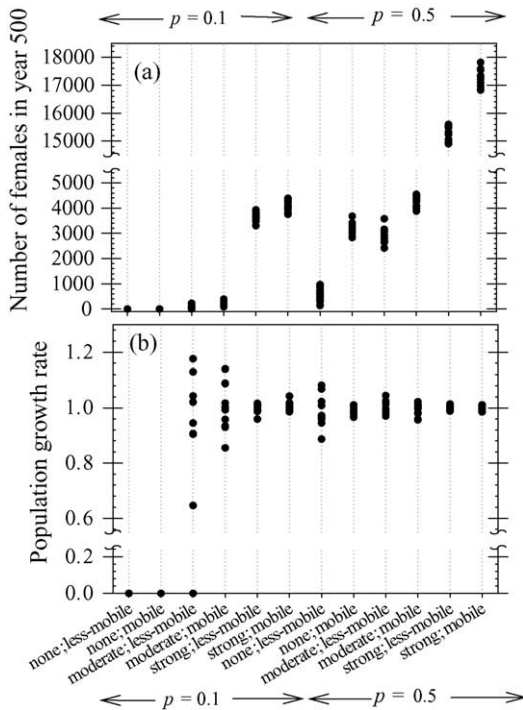
Fig. 6. Predictions of (a) final number of females (N_f) and (b) population growth rate were generated by the PATCH model for ten replicate landscapes in each of nine landscape categories. Landscape categories included two proportions of suitable habitat: rare ($p = 0.1$) and half ($p = 0.5$), and three levels of spatial autocorrelation: none ($C = 0$), moderate ($C = 0.5$), and strong ($C = 1$).
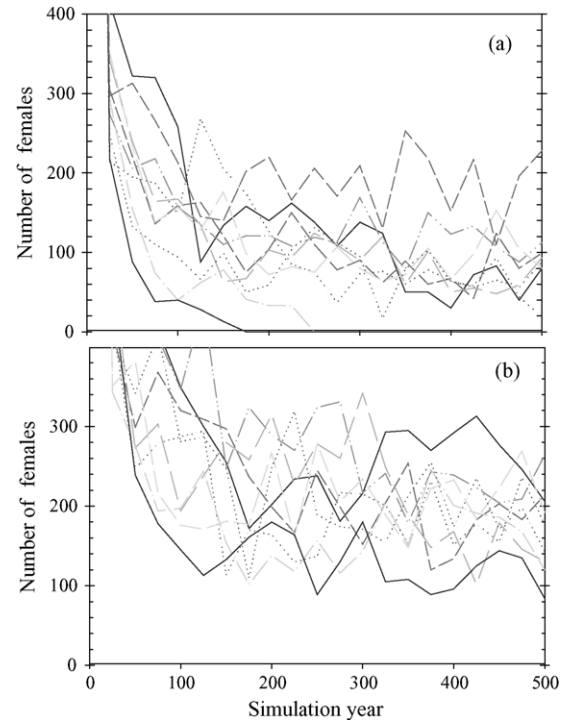

Fig. 7. PATCH simulations of female population size over time on 10 replicate landscapes with rare ($p = 0.1$), locally suitable habitat and moderate spatial autocorrelation ($C = 0.5$) for (a) a less-mobile species and (b) a mobile species.

of locations in the conditioning sample, our method pins the gross features of the alternative landscapes to the original map. Unlike random maps, our maps preserve the spatial orientation of larger patches in the original map because the conditioning sample tends to seed these larger patches. Our approach does not, however, go so far as to analyze and mimic error in the process used to create the original map (Jager and King, 2004). GIS data rarely come with the metadata needed to develop an error budget, which is a significant undertaking in its own right. Instead, our approach estimates map-to-map variation from the geostatistical properties of a single original map that is typically available.

Our results highlight two statistical properties of categorical spatial data. First, variation among landscapes is higher in uncorrelated landscapes than in correlated landscapes, and higher in landscapes with equal pro-

portions of suitable and unsuitable habitat. By extension, for maps with more than two categories, we would expect the highest average uncertainty when the reference map has equal proportions in each category. Second, spatial uncertainty is higher near the boundaries of patches in the original landscape than in the middle of its large patches. McGwire and Fisher (2001) compare two maps describing the spatial uncertainty generated by a method similar to ours describing differences between LANDSAT-classified and ground-truth data. Although they conclude that the two are clearly different, we observe that both maps share this tendency toward higher uncertainty near boundaries.

4.2. Future directions in methodology

We envision two directions for future research to improve the technique proposed here for spatial uncertainty analysis. First, our method for generating spatial

uncertainty does not preserve the patch-size distribution of reference landscapes. Our generated landscapes tend to be highly fragmented near the boundaries of large patches, and they tend not to have inclusions (small patches) within the interior of large patches. Keitt et al. (1997) suggested that overestimation of small patches is a real feature of error in classified imagery. This artificial fragmentation might be reduced by designing a heuristic swapping algorithm to bring the patch-size distribution of generated landscapes close to that of the original landscape. Johnson et al. (1999) suggested that a technique for minimizing differences between conditional frequency distributions of simulated and actual multinomial landscapes could be developed in future.

Another need that we perceive for uncertainty analysis of categorical data is to develop a method that accounts for the hierarchical structure in land cover classification. An approach that first generates higher-level classes and then generates the sub-classes within them would account for the fact that two sub-classes are less likely to be mistaken for one-another if they belong to different classes. For example, first classify patches as forest or grassland; then, classify areas within forest patches as deciduous or coniferous forest, and areas within grassland patches as tallgrass or shortgrass prairie.

4.3. Effects of spatial uncertainty on model predictions

We were surprised by the lack of influence that spatial uncertainty in input data had on predictions of the source–sink model. Compared with the influence of mean spatial properties, the influence of uncertainty was very small. One reason may be that the model uses aggregate summaries of spatial data rather than simulating space explicitly.

Spatial uncertainty produced larger variation in predictions of the PATCH model. Results for this model suggests to us that the effects of spatial uncertainty are mediated by the size of the basin of attraction for model predictions. Consider three cases: (1) situations when the amount of suitable habitat and its spatial arrangement are such that a populations of a species cannot persist, (2) situations when populations saturate the habitat, reaching a size that is not vulnerable to extinction, and (3) situations when habitat capacity is low,

and populations increase or decrease slowly enough that neither absorbing state is reached by the end of the simulation's time horizon.

Case 1: When the amount and arrangement of suitable habitat are such that this species cannot persist, variation among alternative landscapes is unimportant, and all landscapes lead to extinction.

Case 2: When the amount and arrangement of suitable habitat are such that habitat capacity is large, variation among alternative landscapes has a small effect, probably because of differences in their carrying capacities. On landscapes with sufficient clustered habitat, variation in persistence is zero, variation in population growth rate is low, and variation in predictions of population size, N_f, is high.

Case 3: When the amount and arrangement of suitable habitat are such that habitat capacity is small, spatial uncertainty has the greatest effect on persistence and population growth rate. When the habitat becomes saturated at a low population size, the population experiences an elevated risk of extinction.

The concept of Minimum Amount of Suitable Habitat (MASH; Hanski et al., 1999) suggests that knowing the amount of habitat available is sufficient for determining the likelihood of persistence. In this study, spatial autocorrelation also had a strong effect on viability predictions. Our results suggest that extinction thresholds can be more precisely defined based on both properties; for example, persistence is possible if spatial autocorrelation $> X$ and suitable habitat $> Y\%$. Near this threshold, the potential effect of spatial uncertainty on predictions of persistence and population growth rate is greatest.

Both population viability models revealed important effects of species' spatial life history on population persistence, but only small differences in how species respond to spatial uncertainty. Spatial uncertainty had negligible effects on two species with contrasting source habitat requirements in the source–sink model. However, simulated populations of the two species showed very different responses to average landscape properties. In particular, viability of the interior species increased with increasing spatial autocorrelation, whereas viability of the edge-dependent species decreased with increasing spatial autocorrelation.

Our results with the PATCH model did not support our hypothesis that less-mobile species are more sensitive to spatial uncertainty than mobile species. Predictions of N_f for the mobile species were always greater than or equal to those for the non-mobile species because non-mobile females had more trouble finding new breeding territories once the populations reached saturation than their mobile counterparts. Only one case resulted in a difference in variation between N_f predictions for the two species. In this case, the average N_f difference placed one species closer to an extinction threshold than the other species. Differences caused by species mobility might be greater in a model that imposes higher movement costs than does PATCH.

These results lead us to speculate that the same processes that shape basins of attraction for population size control the effects of spatial uncertainty. We speculate that life history attributes and environments that produce complex dynamics are most sensitive to spatial uncertainty. Populations in habitats that promote chaotic population dynamics are likely to show very high sensitivity to slight shifts in demographic parameters associated with the details of a particular landscape. Although the case studies presented here are merely illustrative, they suggest interesting patterns to guide future research in this area.

Appendix A

A.1. Source–sink model

We use a simple two-box spatially implicit model to describe the population dynamics of individuals breeding in source and sink habitat (Pulliam, 1988), with migration between the two habitat types (Pulliam, 1996). Source habitat serves as a net exporter of animals and has a finite rate of population increase greater than one. Sink habitat has a finite rate of population increase less than one that would lead to local extinction in the absence of immigration. This model is given by Eq. (3), where $n^{(1)}$ is the number of breeders in the source habitat; $n^{(2)}$ is the number of breeders in the sink habitat; λ_1 is the finite rate of population increase in source habitat; k_1 is the maximum number of breeders in the source habitat. Parameters λ_2 and k_2 are the corresponding quantities for sink habitat.

$$n_{t+1}^{(1)} = \max \left\{ \begin{pmatrix} \lambda_1 n_t^{(1)}, & n_t^{(1)} \leq k_1 \\ \lambda_1 n_t^{(1)} - (n_t^{(1)} - k_1), & n_t^{(1)} > k_1 \end{pmatrix}, 0 \right\}$$

$$n_{t+1}^{(2)} = \max \left\{ \begin{pmatrix} \lambda_2 n_t^{(2)}, & n_t^{(1)} \leq k_1 \\ \lambda_2 n_t^{(2)} + (n_t^{(1)} - k_1), & n_t^{(1)} > k_1 \end{pmatrix}, 0 \right\}$$

$$(3)$$

Excess breeders in the source habitat emigrate to the sink habitat when $n_t^{(2)} > k_1$. The overall rate of population increase is given by:

$$\lambda = \frac{\lambda_1 n_t^{(1)} + \lambda_2 n_t^{(2)}}{n_t^{(1)} + n_t^{(2)}} \tag{4}$$

The overall population cannot grow ($\lambda > 1$) unless the ratio of source to sink population sizes, R, is above a threshold value,

$$R^* = \frac{\lambda_1 - 1}{1 - \lambda_2}. $$

Although the spatial aspects of this model are minimal, we include space implicitly as habitat area by placing constraints on suitable habitat that could function as source habitat. We defined source habitat for two hypothetical species with different "juxtapositional" habitat requirements. In other words, for each species it is not enough to know that a particular cell is suitable. To serve as source habitat, it must also occur in a required juxtaposition with other suitable or unsuitable habitat. We represent an edge-dependent species that requires habitat within 60 m of the edge of suitable habitat, and an interior species that requires a minimum core patch area of at least 3600 m^2. A 20 m × 20 m cell of suitable habitat is considered edge habitat if it is within 60 m of unsuitable habitat. Otherwise, we consider it core (interior) habitat. A cell is considered sink habitat if it is suitable except that it occurs in the wrong juxtaposition to other habitat. For example, a cell that has $I = 1$, but does not occur within 60-m of an edge is considered a sink for an edge-dependent species.

For each species, we calculate the area of source and sink habitat by using FRAGSTATS (McGarigal and Marks, 1995). Source habitat is assigned a local population growth rate of $\lambda_1 = 1.3$; sink habitat is assigned a population growth rate of $\lambda_2 = 0.8$. We assume that populations completely avoid areas of unsuitable habitat ($I = 0$). We reduce the number of parameters to a manageable number by assuming that equilibrium densities in source and sink habitats are equal. This makes it possible to calculate the overall population growth rate, λ, as a function of the growth rate in each habitat type, and the areas of source, A_1, and sink habitat, A_2:

$$\lambda = \frac{\lambda_1 A_1 + \lambda_2 A_2}{A_1 + A_2} \tag{5}$$

With this modification of the model in (3) and (4), we can explore the effects of spatial uncertainty on the areas of source and sink habitat and the resulting impact on overall population growth rate. We compare variation among model predictions for ten generated landscapes representing each of the six reference landscapes and each of the two species with different source habitat requirements.

A.2. PATCH model

The PATCH model (Schumaker, 1998; Schumaker et al., 2004) is spatially explicit—it represents the habitat as a georeferenced grid of cells that differ in quality, and represent the activities of individual animals on the grid. PATCH links habitat maps with data on species' habitat preferences, territory size, vital rates, and movement ability. The model uses an annual time step to simulate survival, breeding, and movement of females, and to predict changes in population size over time.

PATCH produces a map of hexagonal breeding territories. We created a territory map with 20,958 hexagons, 12 pixels per side, from each replicate landscape for each of the six landscape types (Table 1). The minimum territory size was 3200 m^2 (eight 400-m^2 pixels). We estimated the maximum territory size as 9600 m^2 (24 pixels) by multiplying the minimum territory size by 3.0, which is the modal ratio of maximum to minimum territory radius of values that we found in a survey of published population viability analyses.

Simulated animals search for suitable and unoccupied breeding sites between years. In our simulations, animals use a random walk strategy midway between completely ignoring the quality of potential territories and always moving to the best (highest quality) breeding territory within the search neighborhood.

We contrast simulations of a mobile and a less-mobile species. Individuals of the less-mobile species search a minimum and maximum distance of 20 m (i.e., adjacent hexagons only), whereas individuals of the mobile species search a minimum distance of 100 m and a maximum distance of 1000 m. We also assign females of the mobile species low site fidelity to ensure that adults search for a new breeding site each year. We assign females of the less-mobile species high site

fidelity to ensure that they remain at the same breeding site indefinitely.

The average habitat quality of a territory influences the survival, reproduction, and movement of its occupant. We assume that both species had two age classes, juvenile and adult, with the same maximum vital rates (survival = 0.5 for juveniles and 0.5 for adults; average fecundity = 3 offspring/female). We chose these values because they result in saturation of the breeding territories for landscapes with spatial–statistical attributes that permit persistence. Each breeding female's vital rate is a product of the maximum rate and the proportion of suitable habitat in her territory.

Simulations begin with 500 adult females, run forward for 500 year, and report two predictions: the number of adult females in the final year, and the time-averaged population growth rate (λ) for each replicate with a non-zero final population. We present the mean and standard error of these responses for ten replicate maps for each species on each of the six landscape types in Fig. 2.

References

Bart, J., 1995. Acceptance criteria for using individual-based models to make management decisions. Ecol. Appl. 5 (2), 411–420.

Bennett, D., Martinez-Meyer, E., Feddema, J., 2000. The effect of measurement error on habitat utilization models. In: Proceedings of the Fourth International Conference on Integrating GIS and Environmental Modeling (GIS/EM4): Problems, Prospects, and Research Needs, Banff, Alberta, Canada, September 2–8, 2000.

Bierkens, M.F.P., Burrough, P.A., 1993. The indicator approach to categorical soil data. I. Theory. J. Soil Sci. 44, 361–368.

Burgess, T.M., Webster, R., 1980. Optimal interpolation and isarithmic mapping of soil properties. I. The semi-variogram and punctual kriging. J. Soil Sci. 31, 333–341.

Cormack, R.M., 1988. Statistical challenges in the environmental sciences: a personal view. J. R. Stat. Soc. A 151, 201–210.

Cressie, N., 1985. Fitting variogram models by weighted least squares. Math. Geol. 17 (5), 563–586.

Dunning Jr., J.B., Stewart, D.J., Danielson, B.J., Noon, B.R., Root, T.L., Lamberson, R.H., Stevens, E.E., 1995. Spatially explicit population models: current forms and future uses. Ecol. Appl. 5, 3–11.

Elith, J., Burgman, M.A., Regan, H.M., 2002. Mapping epistemic uncertainties and vague concepts in predictions of species distribution. Ecol. Model. 157, 313–329.

Gardner, R.H., O'Neill, R.V., Mankin, J.B., Carney, J.H., 1981. Comparison of sensitivity analysis and error analysis based on a stream ecosystem model. Ecol. Model. 12, 173–190.

Gardner, R.H., Gustafson, E.J., 2004. Simulating dispersal of reintroduced species within heterogeneous landscapes. Ecol. Model. 171, 339–358.

Gomez-Hernandez, J.J., Srivastava, R.M., 1990. An ANSI-C three-dimensional multiple indicator conditional simulation program. Comput. Geosci. 16 (4), 395.

Gomez-Hernandez, J.J., Cassiraga, E.F., 1994. Theory and practice of sequential simulation. In: Armstrong, M., Dowd, P.A. (Eds.), Geostatistical Simulations. Kluwer Academic Publishers, Dordrecht, pp. 111–124.

Gotway, C., Rutherford, B.M., 1994. Introduction: stochastic simulation for imaging spatial uncertainty: comparison and evaluation of available algorithms. In: Armstrong, M., Dowd, P.A. (Eds.), Geostatistical Simulation. Kluwer Academic Publishers, Dordrecht, pp. 1–12.

Hanski, I., Moilanen, A., Gyllenberg, M., 1999. Minimum viable metapopulation size. Am. Nat. 147 (4), 527–541.

Harris, D.D., Hubert, W.A., Wesche, T.A., 1992. Habitat use by young-of-year brown trout and effects on weighted usable area. Rivers 3 (2), 99–105.

Hansen, A.J., Rotella, J.J., Kraska, M.P.V., Brown, D., 1999. Dynamic habitat and population analysis: an approach to resolve the biodiversity manager's dilemma. Ecol. Appl. 9 (4), 1459–1476.

Heuvelink, G.B.M., 1998. Uncertainty analysis in environmental modelling under a change of spatial scale. Nutrient Cycl. Agroecosyst. 50 (1–3), 255–264.

Hunsaker, C.T., Goodchild, M.F., Friedl, M.A., Case, T.J. (Eds.), 2001. Spatial Uncertainty in Ecology: Implications for Remote Sensing and GIS Applications. Springer, New York.

Isaaks, E.H., 1984. Indicator simulation: application to the simulation of a high grade uranium mineralization. In: Geostatistics for Natural Resources Characterization, Part II. D. Reidel Publishing Co, pp. 45–53.

Jager, H.I., King, A.W., 2004. Spatial uncertainty analysis: methods to evaluate ecological model predictions driven by spatial data. Ecosystems 7, 1–7.

Johnson, G.D., Myers, W.L., Patil, G.P., 1999. Stochastic generating models for simulating hierarchically structured multi-cover landscapes. Landscape Ecol. 14, 413–421.

Journel, A.G., Huijbregts, C.J., 1978. Mining Geostatistics. Academic Press, New York, 600.

Keitt, T.H., Urban, D.L., Milne, B.T., 1997. Detecting critical scales in fragmented landscapes. Conserv. Ecol. 1 (1), 4, URL: http://www.consecol.org/vol1/iss1/art4.

Levins, R.C., 1968. Evolution in Changing Environments: Some Theoretical Explorations. Princeton University Press, Princeton, NJ, 120.

McCarthy, M.A., Burgman, M.A., Ferson, S., 1995. Sensitivity analysis for models of population viability. Biol. Conserv. 73, 93–100.

McGarigal, K., Marks, B.J., 1995. FRAGSTATS: spatial pattern analysis program for quantifying landscape structure. Gen. Tech. Rep. PNW-GTR-351, Forest Service, Pacific Northwest Research Station, Portland, OR.

McGwire, K.C., Fisher, P., 2001. In: Hunsaker, C.T., Goodchild, M.F., Friedl, M.A., Case, T.J. (Eds.), Spatial Uncertainty in Ecology: Implications for Remote Sensing and GIS Applications. Springer, New York, pp. 308–329.

Neuman, S.P., Jacobson, E.A., 1984. Analysis of non-intrinsic spatial variability by residual kriging with application to regional groundwater levels. Math. Geol. 16 (5), 499–521.

Pebesma, E.J., Wesseling, C.G., 1998. Gstat, a program for geostatistical modelling, prediction and simulation. Comput. Geosci. 24 (1), 17–31.

Pulliam, H.R., 1988. Sources, sinks, and population regulation. Am. Nat. 132, 652–661.

Pulliam, H.R., 1996. Sources and sinks: empirical evidence and population consequences. In: Rhodes Jr., O.E., Chesser, R.K., Smith, M.H. (Eds.), Population Dynamics in Ecological Space and Time. The University of Chicago Press, Chicago, pp. 45–69.

Ritchie, M.E., 1997. Populations in a landscape context: sources, sinks and metapopulations. In: Bissonette, J.A. (Ed.), Wildlife and Landscape Ecology: Effects of Pattern and Scale. Springer-Verlag, New York, pp. 160–184.

Rossi, R.E., Borth, P.W., Tollefson, J.J., 1993. Stochastic simulation for characterizing ecological spatial patterns and appraising risk. Ecol. Appl. 3, 719–735.

Schumaker, N.H., 1998. A Users Guide to the PATCH Model. EPA/600/R-98/135. U.S. Environmental Protection Agency, Environmental Research Laboratory, Corvallis, Oregon, 120.

Schumaker, N.H., Ernst, T., White, D., Baker, J., Haggerty, P., 2004. Projecting wildlife responses to alternative future landscapes in Oregon's Willamette Valley. Ecol. Appl. 14 (2), 381–400.

Warrick, A.W., Meyers, D.E., 1987. Optimization of sampling locations for variogram calculations. Water Resour. Res. 23 (3), 496–500.

With, K.A., King, A.W., 2001. Analysis of landscape sources and sinks: the effect of spatial pattern on avian demography. Biol. Conserv. 100, 75–88.